ARTICLES

Mechanism of auxin perception by the TIR1 ubiquitin ligase

Xu Tan[1], Luz Irina A. Calderon-Villalobos[2], Michal Sharon[3], Changxue Zheng[1], Carol V. Robinson[3], Mark Estelle[2] & Ning Zheng[1]

Auxin is a pivotal plant hormone that controls many aspects of plant growth and development. Perceived by a small family of F-box proteins including transport inhibitor response 1 (TIR1), auxin regulates gene expression by promoting SCF ubiquitin-ligase-catalysed degradation of the Aux/IAA transcription repressors, but how the TIR1 F-box protein senses and becomes activated by auxin remains unclear. Here we present the crystal structures of the *Arabidopsis* TIR1–ASK1 complex, free and in complexes with three different auxin compounds and an Aux/IAA substrate peptide. These structures show that the leucine-rich repeat domain of TIR1 contains an unexpected inositol hexakisphosphate co-factor and recognizes auxin and the Aux/IAA polypeptide substrate through a single surface pocket. Anchored to the base of the TIR1 pocket, auxin binds to a partially promiscuous site, which can also accommodate various auxin analogues. Docked on top of auxin, the Aux/IAA substrate peptide occupies the rest of the TIR1 pocket and completely encloses the hormone-binding site. By filling in a hydrophobic cavity at the protein interface, auxin enhances the TIR1–substrate interactions by acting as a 'molecular glue'. Our results establish the first structural model of a plant hormone receptor.

Auxin has long been recognized as an important phytohormone that regulates plant growth in response to diverse developmental and environmental cues[1,2]. The major naturally occurring auxin, indole-3-acetic acid (IAA), coordinates many plant growth processes by modulating gene expression, which leads to changes in cell division, elongation and differentiation. How the auxin signal is perceived and interpreted by plant cells has been a central question in plant biology.

Recent genetic and molecular studies in *Arabidopsis* have revealed a crucial intracellular auxin signalling pathway in which a ubiquitin-dependent proteolytic system has a key role in sensing and transducing the hormone signal to transcriptional programs[3]. At the centre of the signalling cascade is the ubiquitin-ligase complex, SCF^{TIR1}, which promotes the ubiquitin-dependent proteolysis of a family of transcriptional regulators known as Aux/IAAs in an auxin-dependent manner[4]. Degradation of the Aux/IAAs activates the auxin response factor (ARF) family of transcription factors, whose activities in regulating auxin responsive genes are otherwise inhibited by the Aux/IAA proteins[5–9]. The *Arabidopsis* genome encodes 29 Aux/IAA proteins[10–12], most of which share a highly conserved degron sequence (called domain II) that can be recognized by the SCF^{TIR1} complex[13–15]. Importantly, two recent studies have revealed that TIR1, the F-box protein subunit of SCF^{TIR1}, functions as a true auxin receptor[16,17]. It has been shown that auxin binds directly to SCF^{TIR1} and promotes the interaction between TIR1 and Aux/IAAs. In *Arabidopsis*, TIR1 and its closest paralogues AFB1 to AFB5 belong to the C3 subfamily of leucine-rich-repeat-containing F-box proteins[18]. Together with TIR1, AFB1 to AFB3 have been found to function as redundant auxin receptors, collectively mediating auxin-regulated responses throughout plant growth and development[19].

Besides IAA, several naturally occurring and many synthetic auxins have been identified. These compounds are chemically diverse, sharing only a planar unsaturated ring and a side chain with a carboxyl group[20]. Despite several hypotheses on the determinants of auxin activity[21,22], how these variable chemical substances elicit a common phytohormone function remains unclear. In addition to IAA, TIR1 has been reported to recognize at least two other synthetic auxin analogues, 1-naphthalene acetic acid (1-NAA) and 2,4-dichlorophenoxyacetic acid (2,4-D)[16,17]. Similarly to IAA, both compounds are able to promote the binding of Aux/IAA proteins to the TIR1 F-box protein. A structural explanation of how TIR1 perceives and is in turn activated by these structurally distinct auxins will help to elucidate the structure–activity relationships of auxins.

Featuring interchangeable substrate receptor subunits, the SCF and SCF-like cullin-RING complexes control a broad spectrum of cellular functions in eukaryotes by ubiquitinating diverse protein substrates[23]. Substrate recognition by known cullin-RING ubiquitin ligases often involves post-translational modification of the substrate, for instance, serine phosphorylation and proline hydroxylation. Auxin-mediated SCF^{TIR1}–substrate interaction represents a new mechanism in which a naturally occurring small molecule directly stimulates the substrate-binding activity of a cullin-RING ubiquitin ligase. The structural basis of this ubiquitin-ligase regulatory mechanism and its implications beyond phytohormone signalling await clarification.

Here we report a series of crystallographic studies of auxin perception and auxin-promoted substrate-binding of the auxin receptor TIR1. Our results reveal the structural mechanism underlying auxin perception by TIR1, suggest a potential role of inositol hexakisphosphate ($InsP_6$) in plant hormone signalling, and indicate a new direction for developing therapeutic drugs that target human ubiquitin ligases.

Auxin enhances TIR1–Aux/IAA interaction

We overexpressed and purified full-length *Arabidopsis* TIR1 in complex with the full-length SCF^{TIR1} adaptor, ASK1, using the baculovirus–insect cell system. Auxin-enhanced TIR1–Aux/IAA interaction was readily detected in a native gel shift assay. Consistent with early studies, we also observed an intrinsic low affinity between TIR1 and the

[1]Department of Pharmacology, University of Washington, School of Medicine, Box 357280, Seattle, Washington 98195, USA. [2]Department of Biology, Indiana University, Bloomington, Indiana 47405, USA. [3]Department of Chemistry, University of Cambridge, Cambridge, CB2 1EW, UK.

bacteria-produced IAA7 protein in the absence of auxin (Supplementary Fig. 1)[16,17]. These results confirm that auxin regulates SCF^{TIR1} by directly promoting the interactions between TIR1 and its polypeptide substrates[16,17].

To increase the substrate affinity of TIR1, auxin might either bind to an allosteric site and induce conformational changes of the F-box protein, or interact with both TIR1 and the Aux/IAA substrate and extend the binding interface between the two polypeptides. To differentiate between these two distinct mechanisms and to reveal how different auxins can bind to and regulate TIR1, we have determined the crystal structures of the *Arabidopsis* TIR1–ASK1 complex alone and in complexes with three auxin compounds as well as an Aux/IAA degron peptide derived from the IAA7 protein, together and separately at resolutions between 1.8 Å and 2.5 Å (Supplementary Table 1).

Overview of the structure

The TIR1–ASK1 complex has a mushroom-shaped structure with the leucine-rich-repeat (LRR) domain of TIR1 being the 'cap' and the F-box motif of TIR1 together with ASK1 forming the 'stem' (Fig. 1a). The spatial arrangement of the domains in the complex is similar to that seen in the human Skp2–Skp1 complex, in which the F-box protein Skp2 also features an LRR domain[24]. When modelled onto the human SCF complex[25], the TIR1–ASK1 complex orients the top surface of the mushroom cap towards the RING subunit of the E3 machinery (Supplementary Fig. 2). With twice as many LRR motifs as Skp2, the LRR domain of TIR1 (TIR1-LRR) folds into a twisted horseshoe-shaped solenoid (Fig. 1). Strikingly, an unexpected $InsP_6$ molecule is found near the centre of the TIR1-LRR fold in close vicinity to the auxin-binding site (Fig. 1).

The TIR1-LRR domain is solely responsible for auxin perception and IAA7 substrate recruitment. A single top surface pocket in TIR1-LRR performs both functions (Fig. 1). Auxin is recognized at the bottom of the pocket through an overall hydrophobic and partially promiscuous binding site that can accommodate variable planar ring structures. A key TIR1 arginine residue (Arg 403) is supported by the nearby $InsP_6$ cofactor and selects the carboxyl group shared by most auxins. Immediately above the auxin-binding site, the highly coiled IAA7 peptide is docked to the upper part of the surface pocket, packing its central hydrophobic consensus motif directly against auxin and completely covering the plant hormone (Fig. 1a). A superposition analysis shows that the structure of the TIR1 LRR domain remains largely unchanged with or without auxins and/or the IAA7 peptide bound.

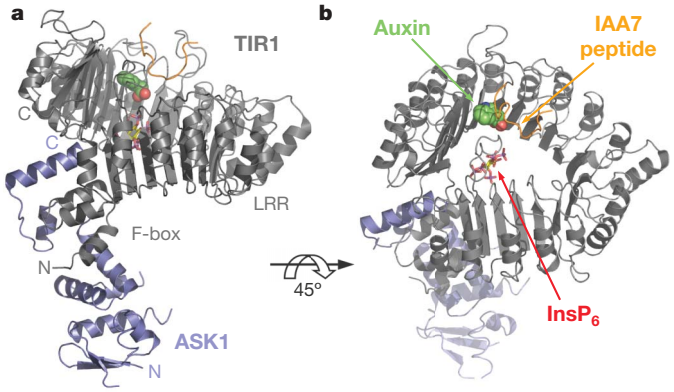

Figure 1 | Crystal structure of the TIR1–ASK1 complex with auxin and the IAA7 degron peptide. **a**, **b**, Two views of the complex structure are shown as a ribbon diagram. TIR1, ASK1 and the IAA7 substrate peptide are coloured grey, blue and orange, respectively. The F-box and LRR domains of TIR1 are labelled. Auxin is represented by a space-filling model (CPK). The $InsP_6$ molecule is shown as a stick model.

Architecture of the TIR1-LRR domain

The TIR1-LRR domain consists of 18 LRRs and a carboxy-terminal cap sequence and adopts an overall architecture that is distinct from other known LRR structures[26]. Each TIR1-LRR contains a β-strand followed by an α-helix. Packing in tandem, the TIR1-LRRs assemble into the expected solenoid structure with an overall horseshoe-like shape. The highly curved solenoid fold is characterized by a concave surface formed mostly by a parallel β-sheet and a convex surface lined with α-helices (Fig. 2a, b). Unlike the regular horseshoe-shaped structures reported for other LRR proteins[27,28], however, the TIR1-LRR solenoid has an abrupt kink in the middle, highlighted by the α-helix of the eighth LRR protruding from the convex surface (Fig. 2a, b). The two halves of the TIR1-LRR horseshoe are packed at an angle and the ends of the horseshoe are close to each other (Fig. 2b). The C-terminal cap sequence, which extends the LRRs by three antiparallel β-strands, is positioned right above the first LRR and essentially closes the curved solenoid as a complete circle. The resulting twisted structure can be likened to a thick 'spring washer', which is overall a one-coil helix (Fig. 2b).

The unique architecture of the TIR1-LRR domain is critical for the function of the auxin receptor. The intra-repeat loops associated with LRRs 2, 12 and 14 are unusually long and located at the top surface of the TIR1-LRR solenoid (Fig. 2). Of the three long loops, the LRR-2 loop (loop-2) plays a pivotal role in constructing the auxin- and substrate-binding surface pocket by interacting with the nearby concave surface of the TIR1-LRR solenoid. This part of the solenoid inner wall is mainly formed by the C-terminal cap sequence and is brought to the close vicinity of the second repeat by the twist in the middle of TIR1-LRR (Fig. 2). With its flanking regions held by the C-terminal cap β-sheet, the central part of loop-2 forms a 3_{10}-helix and approaches the concave surface and the other two long loops at the opposite side of the solenoid. Together, the three long loops and the nearby concave surface of the twisted LRR fold form the auxin- and substrate-binding pocket (Fig. 2c).

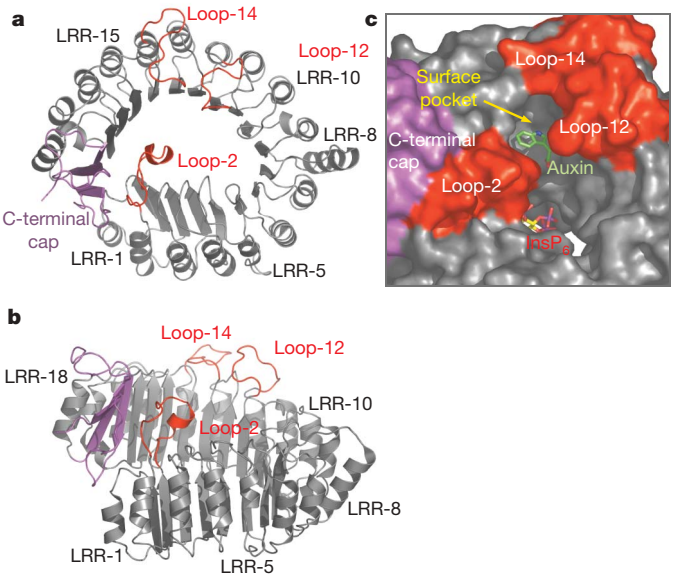

Figure 2 | Architecture of the TIR1-LRR domain. **a**, **b**, Two orthogonal views of the LRR domain of TIR1. The eighteen LRR motifs are numbered and shown in grey. The C-terminal cap sequence is shown in magenta. The three substrate-contacting top surface loops in LRR-2, LRR-12 and LRR-14 are shown in red and labelled as loop-2, loop-12 and loop-14. **c**, Surface representation of the TIR1-LRR domain, focusing on the auxin- and substrate-binding pocket created by the intra-repeat loop of LRR-2 (loop-2), which packs against the concave surface of the LRR solenoid. The TIR1-bound auxin and the nearby $InsP_6$ are represented as stick models.

Identification of $InsP_6$ in TIR1

In addition to an unusual architecture, the TIR1-LRR domain is distinct from other LRR proteins in having a previously unknown co-factor tightly bound near the centre of the solenoid fold. Crystallographic analysis of the TIR1–ASK1 complex at 1.8 Å resolution reveals an island of unexplained electron density under the 3_{10}-helix of loop-2. Surrounded by numerous residues on the concave surface of the TIR1-LRR domain, the extra density is characterized by six similarly sized branches, all connected to a central body (Fig. 3a).

The distinctive features of the unexpected electron density strongly suggest that it belongs to an $InsP_6$ molecule co-purified with the TIR1–ASK1 protein complex from insect cells. A myo-inositol-1,2,3,4,5,6-hexakisphosphate molecule would have a well matched electron density pattern and this would also explain its close interactions with a highly basic surface area of TIR1 (Fig. 3b), which consists of ten positively charged TIR1 residues (Fig. 3a). In addition, mass spectrometry analysis shows that the observed molecular weight of the unknown molecule is essentially identical to the calculated molecular weight of $InsP_6$, unequivocally confirming its chemical identity (Supplementary Fig. 3). The properties of the inositol-hexakisphosphate-binding site and its spatial relationship to the nearby auxin-binding site in TIR1 suggest that $InsP_6$ is probably a structural co-factor of the auxin receptor (see below).

The TIR1 auxin-binding pocket

As revealed in both structures of TIR1–IAA and TIR1–IAA–Aux/IAA degron peptide, TIR1 recognizes auxin through the bottom portion of the surface pocket formed between the LRR-2 loop and the solenoid inner surface. Facing towards the central channel of the LRR solenoid, the pocket is analogous to a three-walled room with an open ceiling (Fig. 2c, 4a). The 3_{10}-helix of loop-2 forms one 'wall', while the highly curved concave surface presented by LRR-12 to LRR-16 defines the other two. The floor of the pocket is made of a layer of residues from both loop-2 and the concave surface (His 78, Arg 403, Ser 438, Ser 462 and Glu 487), together with a water molecule sequestered in the middle (Fig. 4a). Below the floor, another layer of TIR1 residues (Arg 436, Met 460 and Lys 485), all interacting with $InsP_6$, supports the pocket from underneath and leaves it accessible only from the top. The integrity of the pocket floor is crucial for auxin binding: one amino-acid mutation (S462E) is sufficient to abolish auxin-enhanced binding but does not inhibit basal substrate binding by TIR1 (Fig. 4c).

IAA, the natural auxin, binds to the base of the TIR1 pocket via two important functional moieties, the side-chain carboxyl group and the indole ring (Fig. 4a and Supplementary Fig. 4). The carboxyl group of IAA anchors the plant hormone to the bottom of the TIR1 pocket by forming a salt bridge and two hydrogen bonds with two residues from the pocket floor (Arg 403 and Ser 438). Meanwhile, the indole ring of IAA stacks on top of the pocket floor with its edge packing against the surrounding walls through hydrophobic interactions and van der Waals contacts. On the loop-2 side of the pocket, the benzene region of the auxin indole ring interacts with two TIR1 phenylalanine residues (Phe 79 and Phe 82). On the concave surface side, the rest of the auxin indole ring is partially sandwiched between two parallel layers of TIR1 residues and is therefore mainly in contact with the TIR1 polypeptide backbone (Fig. 4b). Unique to IAA, a hydrogen bond is donated by the NH group of the auxin indole ring to a nearby carbonyl group, which belongs to the backbone of a slightly twisted TIR1 β-strand (Fig. 4a, d).

Despite having different ring structures, the two synthetic auxin analogues 1-NAA and 2,4-D bind to TIR1 in a manner similar to that of IAA (Fig. 4d). Through a common carboxyl group, both auxin analogues are tethered to the floor of the TIR1 pocket. The naphthalene ring of 1-NAA, which is slightly larger than an indole ring, is placed in the cavity with an orientation almost identical to the auxin indole ring. The dichlorophenyl ring of 2,4-D fits into the pocket base with its widest dimension (defined by the two large chlorines) aligned with that of the pocket, thus mimicking the double-rings of the other two auxin compounds (Fig. 4d). In both cases, the ring structure of the compound is accommodated by the overall shape and generally hydrophobic properties of the TIR1 cavity. The auxin-binding site of TIR1 is therefore defined by two highly selective polar residues

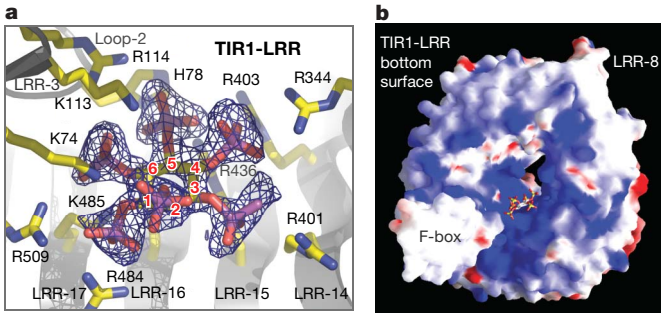

Figure 3 | $InsP_6$ as a TIR1 co-factor. **a**, A close-up view of the TIR1-bound $InsP_6$. The $InsP_6$ molecule is shown as a stick model, together with its positive $F_o - F_c$ electron density calculated and contoured at 4σ before it was built into the TIR1 model. TIR1 residues that are in direct contact with $InsP_6$ are shown as a stick model. **b**, Electrostatic surface potential of the TIR1-LRR bottom surface: positive (blue) to negative (red). The F-box domain and LRR-8 of TIR1 are labelled to indicate the orientation of the domain.

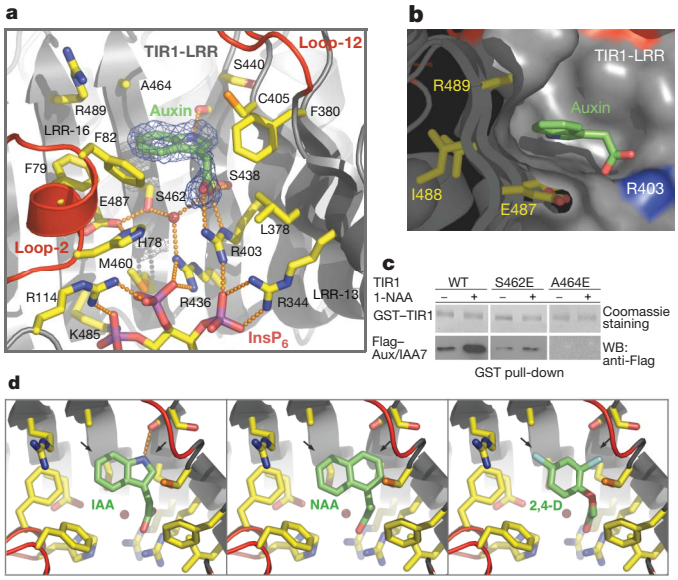

Figure 4 | Recognition of auxin by TIR1. **a**, A close-up view of the auxin-binding site with its nearby $InsP_6$ molecule. The auxin molecule (IAA) is shown as a green stick model, together with its positive $F_o - F_c$ electron density calculated and contoured at 3σ before it was built into the complex model. The TIR1 residues surrounding auxin and right underneath the auxin-binding site are shown as a yellow stick model. A central water molecule as part of the pocket floor is shown as a red sphere. The hydrogen-bond and salt-bridge network connecting auxin and $InsP_6$ are indicated by orange dashed lines. **b**, A slab view of the TIR1 cavity accommodating the auxin indole ring. The TIR1-LRR domain is in surface representation. Three layers of TIR1 residues defining a wall for the auxin-binding site are modelled as sticks. Arg 403 interacts with the auxin carboxyl group and is coloured blue. **c**, GST pull-down assay with (+) or without (−) 50 μM 1-NAA. In the upper panel, purified recombinant wild type (WT) or mutants GST–TIR1 are visualized by Coomassie staining for loading control. In the lower panel, Flag-tagged IAA7 pulled down by GST–TIR1 was detected by western blot. **d**, A top view of the TIR1 cavity with IAA, 1-NAA and 2,4-D bound. The three auxin analogues are all shown as green stick models. In each panel, two black arrows indicate the widest dimension of each compound.

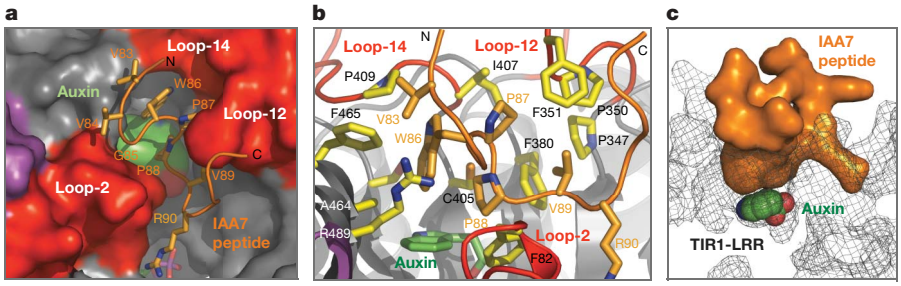

Figure 5 | Binding of an Aux/IAA degron peptide on auxin-bound TIR1. **a**, An overall view of the TIR1 surface pocket occupied by auxin (green) at the bottom and the highly coiled IAA7 peptide (orange) on top. The surface of the three long top surface loops of TIR1 responsible for ligand binding is coloured red. **b**, A close-up side view of the central GWPPV motif in the IAA7 peptide upon binding to TIR1. Interacting residues of the substrate peptide and TIR1 are shown as orange and yellow stick models, respectively. Auxin is shown as a green stick model. To clarify the view, two hydrophobic residues, one from the peptide and the other from loop-2 of TIR1, are not shown. **c**, A slab view of the TIR1–auxin–IAA7 peptide complex, showing that auxin fills a cavity between two proteins. The molecular surface of TIR1 is shown in grey mesh. The IAA7 peptide and auxin are shown in orange surface representation and green CPK, respectively.

(Arg 403 and Ser 438) spatially coupled to a less selective hydrophobic cavity with a fixed shape. This partially promiscuous hormone-binding site in TIR1 explains how the auxin receptor can potentially bind a variety of auxin compounds.

TIR1–substrate peptide interactions

The IAA7 degron peptide has a predominantly hydrophobic sequence and binds to the auxin-bound TIR1 pocket through extensive hydrophobic interactions (Fig. 5a, b). The mouth of the TIR1 pocket is formed mostly by the three extra long LRR loops and is decorated almost exclusively with hydrophobic residues (Fig. 5b). In between the pocket opening and the auxin molecule, another layer of TIR1-LRR residues presents an additional hydrophobic surface. The 13-amino-acid substrate peptide adopts a highly coiled conformation and fills the TIR1 pocket with the central hydrophobic consensus motif GWPPV lying on top of auxin (Fig. 5a, b). The two flanking regions of the motif also contribute to complex formation. The hydrophobic amino-terminal region runs along the pocket rim and the polar C-terminal region curls around the LRR-12 loop of TIR1 (Fig. 5a).

The conserved central GWPPV motif represents the hallmark of the Aux/IAA degron[13]. Genetic screens in *Arabidopsis* have shown that mutations in this motif lead to stabilization of Aux/IAAs and reduced auxin response. Two amino acids in the motif, tryptophan and the second proline, interact with the surrounding hydrophobic wall of the TIR1 pocket and stack against the auxin molecule lying underneath, packing against the auxin indole ring and the auxin side chain, respectively (Fig. 5b and Supplementary Fig. 4). The positions of these two residues are partially maintained by the other proline in the middle, which itself also forms hydrophobic interactions with surrounding TIR1 residues. Similar to the three central residues of the motif, the glycine residue at the first position is invariant among all Aux/IAAs[13]. In the structure, the glycine residue is located at a critical position, where flexibility of the peptide is required for the N-terminal region of the substrate peptide to take a sharp turn and continue interacting with TIR1 (Fig. 5a). Although the valine residue at the end of the motif is not strictly conserved in all Aux/IAA family members, its conserved hydrophobic feature is crucial for its interactions with the nearby hydrophobic residues of TIR1 (Fig. 5b). As a whole, the GWPPV motif of the substrate peptide, together with auxin, nucleates a hydrophobic core networked with the TIR1 hydrophobic surface pocket. When a single non-polar TIR1 residue in the pocket is altered to a charged amino acid (A464E), both the basal and auxin-enhanced binding of the IAA7 substrate to TIR1 are lost (Fig. 4c).

Upon docking to auxin-bound TIR1, the IAA7 peptide almost completely encloses the three-walled TIR1 pocket, covering both its open 'ceiling' and the empty side facing the central channel of the LRR solenoid (Fig. 5a). Thus, the receptor-bound hormone is expected to remain trapped in the pocket until the substrate polypeptide is released. Overall, even though the Aux/IAA substrate itself does not have any detectable affinity to auxin, an optimal binding site for the hormone is cooperatively formed by the substrate polypeptide and TIR1.

Auxin regulation of TIR1–Aux/IAA binding

The crystal structure of TIR1–ASK1 in the ligand-free and different ligand-bound forms reveals that auxin is not an allosteric regulator of SCF^{TIR1}. Superposition analysis of the TIR1–ASK1 structures in the absence and presence of auxin shows that except for the side-chain rearrangement of three local residues (Supplementary Fig. 5), auxin binding does not induce significant conformational changes of the hormone receptor. Furthermore, the auxin-binding site is disqualified as an allosteric site because it is in the same pocket as the substrate-binding site.

Instead, auxin enhances the substrate-binding activity of TIR1 mainly by filling a cavity between the two proteins, thereby extending the protein-interaction interface. Upon interacting with both TIR1 and the substrate polypeptide, auxin mediates the formation of a continuous hydrophobic core among the three. Thus, we conclude that auxin promotes SCF^{TIR1}–substrate binding by acting as a 'molecular glue' rather than an allosteric switch (Fig. 6). Such a regulatory mechanism is in fact consistent with the partially promiscuous nature of auxin binding to the F-box protein. Because the structural role of auxin is to support the GWPPV motif of the Aux/IAA substrate by providing an overall hydrophobic base at the bottom of the TIR1 surface pocket, moderate variations in auxin structure might be tolerated as long as they can be accommodated by the auxin-binding site and do not interfere with Aux/IAA binding.

$InsP_6$ as a possible co-factor of TIR1

$InsP_6$, also known as "phytate", was first identified in plants and later found in other eukaryotes[29]. Many lines of evidence indicate that the $InsP_6$ revealed in the crystals is a specific functional cofactor of TIR1.

Figure 6 | A model of auxin-regulated TIR1–substrate interactions. A schematic diagram of auxin functioning as a 'molecular glue' to enhance TIR1–substrate interactions. In contrast to an allosteric mechanism, auxin binds to the same TIR1 pocket that docks the Aux/IAA substrate. Without inducing significant conformational changes in its receptor, auxin increases the affinity of two proteins by simultaneously interacting with both in a cavity at the protein interface.

First, the robust co-purification of $InsP_6$ with the TIR1–ASK1 complex through multiple steps of purification shows that the $InsP_6$ is tightly associated with TIR1. Second, eight out of the ten positively charged TIR1 residues that interact with $InsP_6$ are strictly conserved among the *Arabidopsis* AFBs (Supplementary Figs 6 and 7), suggesting that $InsP_6$-binding is essential for this specific subfamily of F-box proteins. Third, the $InsP_6$ molecule interacts with several structural elements of TIR1 that are functionally important. These include both halves of the TIR1-LRR solenoids, loop-2 and Arg403 (Fig. 1b and 3a).

Our discovery of the presence of $InsP_6$ in TIR1 represents the second time $InsP_6$ has been identified in a protein structure via X-ray crystallography[30]. On the basis of a number of other studies, $InsP_6$ has now been shown to regulate a variety of cellular functions such as DNA repair, chromatin remodelling, endocytosis and nuclear messenger RNA export[31–34]. Although the essential role of $InsP_6$ in the *Arabidopsis* auxin receptor TIR1 remains to be confirmed, future studies might elucidate how auxin signalling potentially interfaces with other plant signalling events that govern $InsP_6$ metabolism.

Biological and pharmacological implications

In plants, multiple phytohormone signalling pathways are now known to be regulated by ubiquitin ligases[35]. In particular, jasmonic acid signalling requires COI1, an F-box protein with high sequence similarity to TIR1[36]. Our structural results predict that COI1 adopts a TIR1-like structure and possibly functions as a jasmonic acid receptor. Most of the auxin-contacting residues in TIR1 are indeed not conserved in COI1 (Supplementary Fig. 6). Although TIR1 orthologues so far are only found in plants, a small ligand-sensing site regulating substrate recruitment could conceivably be evolved in a different structural context in other eukaryotic ubiquitin ligases.

An increasing number of human disorders has now been associated with defective ubiquitin-ligase–substrate interactions owing to mutations of the ligases themselves, ubiquitination substrates or upstream signalling proteins responsible for substrate priming[37]. The regulatory mechanism of TIR1 by auxin suggests that it is possible for small molecules to promote protein–protein interactions in ubiquitin ligases. Developing protein interaction agonists could potentially resurrect the disease-causing defective ubiquitination processes. Further studies following this principle may open up the development of pharmaceutical agents targeting ubiquitin ligases and potentially other protein interaction systems that are impaired by genetic alterations.

METHODS

Protein preparation and GST pull-down assay. The full-length *Arabidopsis thaliana* TIR1 and ASK1 were co-expressed as a glutathione S-transferase (GST)-fusion protein and a 6X His-tag fusion protein, respectively, in Hi5 suspension insect cells. The TIR1–ASK1 complex was isolated from the soluble cell lysate by glutathione affinity chromatography. After cleavage by TEV, the complex was further purified by anion exchange and gel filtration chromatography and concentrated by ultrafiltration to 4 mg ml^{-1}. GST pull-down assays were carried out using affinity-purified recombinant GST–TIR1–ASK1 (insect cells) and His-Flag-tagged IAA7 proteins (*Escherichia coli*).

Crystallization and data collection. The TIR1–ASK1 crystals were grown at 25 °C by the hanging-drop vapour-diffusion method with 1.5 μl protein samples mixed with an equal volume of reservoir solution containing 100 mM BTP (pH = 6.0), 10–14% PEG 20,000, 200 mM NaCl and 5 mM DTT. Diffraction-quality crystals were obtained by macro-seeding at 4 °C. The crystals form in space group $C2$ ($a = 102.5$ Å, $b = 80.5$ Å, $c = 125.0$ Å, $\alpha = \gamma = 90°$, $\beta = 105.1°$) and contain one molecule in the asymmetric unit. The TIR1–ASK1 derivative crystals were prepared by soaking the native crystal in the reservoir solution supplemented with 16 compounds containing Hg, Au and Pt for 2 h. Among them, five compounds (thimerasol, $(NH_4)_2PtCl_4$, K_2PtCl_6, K_2PtCl_4 and $KAu(CN)_2$) produced diffracting crystals that are isomorphous to the native crystals and were used for data collection. The TIR1–ASK1 crystals were also soaked with different auxins (IAA, 2,4-D and NAA, from Sigma) and an Aux/IAA peptide (NH2-QVVGWPPVRNYRK-COOH) to obtain complex crystals (see Supplementary Table 1). The data sets were collected at the BL8.2.1, BL8.2.2, BL5.0.1 and BL5.0.3 beamlines at the Advanced Light Source in Berkeley, using crystals flash-frozen in the crystallization buffers supplemented with 15–20% glycerol at −170 °C.

Crystal structure determination. The TIR1–ASK1 structure was determined by the multiple-isomorphous-replacement method using native crystals and the five heavy-metal-compound-derived crystals mentioned above. All data sets were integrated and scaled using HKL2000[38]. A single multiple-isomorphous-replacement solution was found using the SOLVE program[39], with several heavy-metal sites located by the program for each derivative crystal. Using this phase information, the structural model was built manually in the program O[40] and refined using the program CNS[41]. Further refinement was done in REFMAC[42] with the TLS program parameters generated by the TLSMD server[43]. The structures of TIR1–ASK1 in complex with different combinations of auxins and AUX/IAA peptide were solved by molecular replacement with the TIR1–ASK1 structure using the Phaser program and refined using CNS and REFMAC.

Received 27 January; accepted 8 March 2007.

1. Woodward, A. W. & Bartel, B. Auxin: regulation, action, and interaction. *Ann. Bot. (Lond.)* **95,** 707–735 (2005).
2. Teale, W. D., Paponov, I. A. & Palme, K. Auxin in action: signalling, transport and the control of plant growth and development. *Nature Rev. Mol. Cell Biol.* **7,** 847–859 (2006).
3. Dharmasiri, N. & Estelle, M. Auxin signaling and regulated protein degradation. *Trends Plant Sci.* **9,** 302–308 (2004).
4. Gray, W. M., Kepinski, S., Rouse, D., Leyser, O. & Estelle, M. Auxin regulates SCF(TIR1)-dependent degradation of AUX/IAA proteins. *Nature* **414,** 271–276 (2001).
5. Hagen, G. & Guilfoyle, T. Auxin-responsive gene expression: genes, promoters and regulatory factors. *Plant Mol. Biol.* **49,** 373–385 (2002).
6. Reed, J. W. Roles and activities of Aux/IAA proteins in *Arabidopsis*. *Trends Plant Sci.* **6,** 420–425 (2001).
7. Liscum, E. & Reed, J. W. Genetics of Aux/IAA and ARF action in plant growth and development. *Plant Mol. Biol.* **49,** 387–400 (2002).
8. Zenser, N., Ellsmore, A., Leasure, C. & Callis, J. Auxin modulates the degradation rate of Aux/IAA proteins. *Proc. Natl Acad. Sci. USA* **98,** 11795–11800 (2001).
9. Tiwari, S. B., Wang, X. J., Hagen, G. & Guilfoyle, T. J. AUX/IAA proteins are active repressors, and their stability and activity are modulated by auxin. *Plant Cell* **13,** 2809–2822 (2001).
10. Remington, D. L., Vision, T. J., Guilfoyle, T. J. & Reed, J. W. Contrasting modes of diversification in the Aux/IAA and ARF gene families. *Plant Physiol.* **135,** 1738–1752 (2004).
11. Overvoorde, P. J. *et al.* Functional genomic analysis of the AUXIN/INDOLE-3-ACETIC ACID gene family members in *Arabidopsis* thaliana. *Plant Cell* **17,** 3282–3300 (2005).
12. Okushima, Y. *et al.* Functional genomic analysis of the AUXIN RESPONSE FACTOR gene family members in *Arabidopsis* thaliana: unique and overlapping functions of ARF7 and ARF19. *Plant Cell* **17,** 444–463 (2005).
13. Ramos, J. A., Zenser, N., Leyser, O. & Callis, J. Rapid degradation of auxin/indole acetic acid proteins requires conserved amino acids of domain II and is proteasome dependent. *Plant Cell* **13,** 2349–2360 (2001).
14. Dharmasiri, N., Dharmasiri, S., Jones, A. M. & Estelle, M. Auxin action in a cell-free system. *Curr. Biol.* **13,** 1418–1422 (2003).
15. Kepinski, S. & Leyser, O. Auxin-induced SCFTIR1-Aux/IAA interaction involves stable modification of the SCFTIR1 complex. *Proc. Natl Acad. Sci. USA* **101,** 12381–12386 (2004).
16. Dharmasiri, N., Dharmasiri, S. & Estelle, M. The F-box protein TIR1 is an auxin receptor. *Nature* **435,** 441–445 (2005).
17. Kepinski, S. & Leyser, O. The *Arabidopsis* F-box protein TIR1 is an auxin receptor. *Nature* **435,** 446–451 (2005).
18. Gagne, J. M., Downes, B. P., Shiu, S. H., Durski, A. M. & Vierstra, R. D. The F-box subunit of the SCF E3 complex is encoded by a diverse superfamily of genes in *Arabidopsis*. *Proc. Natl Acad. Sci. USA* **99,** 11519–11524 (2002).
19. Dharmasiri, N. *et al.* Plant development is regulated by a family of auxin receptor F box proteins. *Dev. Cell* **9,** 109–119 (2005).
20. Jonsson, A. *Encyclopaedia of Plant Physiology* **14,** 959–1006 (Springer, Berlin, 1961).
21. Kaethner, T. Conformational change theory for auxin structure-activity relationships. *Nature* **267,** 19–23 (1977).
22. Farrimond, J. A., Elliott, M. C. & Clack, D. W. Charge separation as a component of the structural requirements for hormone activity. *Nature* **274,** 401–402 (1978).
23. Petroski, M. D. & Deshaies, R. J. Function and regulation of cullin-RING ubiquitin ligases. *Nature Rev. Mol. Cell Biol.* **6,** 9–20 (2005).
24. Schulman, B. A. *et al.* Insights into SCF ubiquitin ligases from the structure of the Skp1-Skp2 complex. *Nature* **408,** 381–386 (2000).
25. Zheng, N. *et al.* Structure of the Cul1-Rbx1-Skp1-F boxSkp2 SCF ubiquitin ligase complex. *Nature* **416,** 703–709 (2002).
26. Kobe, B. & Kajava, A. V. The leucine-rich repeat as a protein recognition motif. *Curr. Opin. Struct. Biol.* **11,** 725–732 (2001).

27. Kobe, B. & Deisenhofer, J. Crystallization and preliminary X-ray analysis of porcine ribonuclease inhibitor, a protein with leucine-rich repeats. *J. Mol. Biol.* **231,** 137–140 (1993).
28. Choe, J., Kelker, M. S. & Wilson, I. A. Crystal structure of human toll-like receptor 3 (TLR3) ectodomain. *Science* **309,** 581–585 (2005).
29. Irvine, R. F. & Schell, M. J. Back in the water: the return of the inositol phosphates. *Nature Rev. Mol. Cell Biol.* **2,** 327–338 (2001).
30. Macbeth, M. R. *et al.* Inositol hexakisphosphate is bound in the ADAR2 core and required for RNA editing. *Science* **309,** 1534–1539 (2005).
31. Hanakahi, L. A., Bartlet-Jones, M., Chappell, C., Pappin, D. & West, S. C. Binding of inositol phosphate to DNA-PK and stimulation of double-strand break repair. *Cell* **102,** 721–729 (2000).
32. Steger, D. J., Haswell, E. S., Miller, A. L., Wente, S. R. & O'Shea, E. K. Regulation of chromatin remodeling by inositol polyphosphates. *Science* **299,** 114–116 (2003).
33. York, J. D., Odom, A. R., Murphy, R., Ives, E. B. & Wente, S. R. A phospholipase C-dependent inositol polyphosphate kinase pathway required for efficient messenger RNA export. *Science* **285,** 96–100 (1999).
34. Hoy, M. *et al.* Inositol hexakisphosphate promotes dynamin I-mediated endocytosis. *Proc. Natl Acad. Sci. USA* **99,** 6773–6777 (2002).
35. Moon, J., Parry, G. & Estelle, M. The ubiquitin-proteasome pathway and plant development. *Plant Cell* **16,** 3181–3195 (2004).
36. Xie, D. X., Feys, B. F., James, S., Nieto-Rostro, M. & Turner, J. G. COI1: an *Arabidopsis* gene required for jasmonate-regulated defense and fertility. *Science* **280,** 1091–1094 (1998).
37. Nalepa, G., Rolfe, M. & Harper, J. W. Drug discovery in the ubiquitin-proteasome system. *Nature Rev. Drug Discov.* **5,** 596–613 (2006).
38. Otwinowski, Z. & Minor, W. (eds) *Processing of X-ray Diffraction Data Collected in Oscillation Mode* (Academic Press, New York, 1997).
39. Terwilliger, T. C. Maximum-likelihood density modification. *Acta Crystallogr. D* **56,** 965–972 (2000).
40. Jones, T. A., Zou, J. Y., Cowan, S. W. & Kjeldgaard, M. Improved methods for building protein models in electron density maps and the location of errors in these models. *Acta Crystallogr. A* **47,** 110–119 (1991).
41. Brunger, A. T. *et al.* Crystallography & NMR system: A new software suite for macromolecular structure determination. *Acta Crystallogr. D* **54,** 905–921 (1998).
42. CCP4. The CCP4 Suite: programs for protein crystallography. *Acta Crystallogr. D* **50,** 760–763 (1994).
43. Painter, J. & Merritt, E. A. Optimal description of a protein structure in terms of multiple groups undergoing TLS motion. *Acta Crystallogr. D* **62,** 439–450 (2006).

Supplementary Information is linked to the online version of the paper at www.nature.com/nature.

Acknowledgements We thank the beamline staff of the Advanced Light Source at Berkeley for help with data collection. We also thank J. Callis, W. Xu and members of the Zheng laboratory for discussions and help. This work is supported by grants from the National Institutes of Health (M.E), the Pew Scholar Program (N.Z.), the National Science Foundation (M.E.) and the Department of Energy (M.E.).

Author Information Structure coordinates and structural factors are deposited in the Protein Data Bank under accession numbers 2P1M, 2P1N, 2P1O, 2P1P and 2P1Q (see Supplementary Table 1). Reprints and permissions information is available at www.nature.com/reprints. The authors declare no competing financial interests. Correspondence and requests for materials should be addressed to N.Z. (nzheng@u.washington.edu).